

# The Reactions of O(<sup>3</sup>P) with Terminal Alkenes: The H<sub>2</sub>CO Channel via 3,2 H-Atom Shift<sup>†</sup>

Hongmei Su,\* Shaolei Zhao, Kunhui Liu, and Tiancheng Xiang

State Key Laboratory of Molecular Reaction Dynamics, and Beijing National Laboratory for Molecular Sciences (BNLMS), Institute of Chemistry, Chinese Academy of Sciences, Beijing 100080, People's Republic of China

Received: May 23, 2007; In Final Form: July 30, 2007

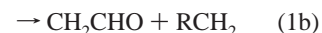
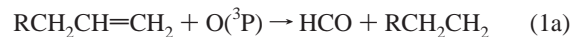
The step-scan time-resolved FTIR emission spectroscopy is used to characterize systematically the H<sub>2</sub>CO channel for the reactions of O(<sup>3</sup>P) with various alkenes. IR emission bands due to the products of CO, CO<sub>2</sub>, and H<sub>2</sub>CO have been observed in the spectra. H<sub>2</sub>CO is identified to be the primary reaction product whereas CO and CO<sub>2</sub> are secondary reaction products of O(<sup>3</sup>P) with alkenes. A general trend is observed in which the fraction yield of the H<sub>2</sub>CO product increases substantially as the reactant alkene varies from C<sub>2</sub>H<sub>4</sub>, C<sub>3</sub>H<sub>6</sub>, 1-C<sub>4</sub>H<sub>8</sub>, iso-C<sub>4</sub>H<sub>8</sub>, to 1-C<sub>5</sub>H<sub>10</sub>. The formation mechanism of the H<sub>2</sub>CO is therefore elucidated to arise from a 3,2 H-atom shift followed by breaking of the C<sub>1</sub>–C<sub>2</sub> bond in the initially formed energized diradical RCH<sub>2</sub>–CHCH<sub>2</sub>O\*. The 3,2 H-atom shift may become the dominant process with the more rapid delocalization of the energy when the hydrocarbon chain of the alkene molecule is lengthened.

## 1. Introduction

Reactions of the oxygen atom with alkenes have been attracting long-time attention constantly due to their importance to atmospheric chemistry and combustion chemistry. The identification of reaction channels is of great help to understand the reaction mechanism and therefore to improve realistic conditions, such as combustion efficiency. As is well-known, small unsaturated hydrocarbons such as C<sub>2</sub>H<sub>2</sub>, C<sub>2</sub>H<sub>4</sub>, C<sub>3</sub>H<sub>4</sub>, and C<sub>3</sub>H<sub>6</sub> are crucial intermediates in hydrocarbon flames.<sup>1,2</sup> These small unsaturated hydrocarbons mainly, if not dominantly, react with triplet ground-state oxygen atoms. These reactions are believed to play key roles in the generation of polycyclic aromatic hydrocarbons and soot.<sup>3</sup> In this work, our main aim is to study the formaldehyde channel of the reactions of O(<sup>3</sup>P) with a series of alkenes.

Dating back to the early 1950s, Cvetanovic and co-workers carried out pioneering studies of the reactions of O(<sup>3</sup>P) with alkenes in the gas phase.<sup>4–10</sup> They found that the reaction proceeds readily with the initial attachment of the electrophilic O atom to the less-substituted carbon atom of the double bond, forming a ketocarbene. In recent years, Bersohn's group performed a series of detailed studies of the reaction products of O(<sup>3</sup>P) with alkenes.<sup>11–15</sup> A general reaction mechanism was suggested in which O(<sup>3</sup>P) initially undergoes an electrophilic addition onto the C=C bond, forming a triplet diradical ketocarbene RCH<sub>2</sub>CHCH<sub>2</sub>O which either decomposes directly to a variety of final products such as vinyloxy CH<sub>2</sub>CHO or carries out intersystem crossing (ISC) to form a singlet diradical. In the singlet state, the barrier to the 1,2 H-atom shift is lowered dramatically, and the energized intermediate can give rise, through the 1,2 H-atom migration and

dissociation, to final products such as HCO. Several channels are identified

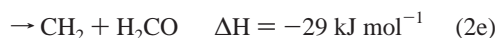
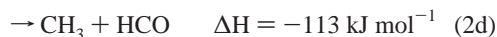
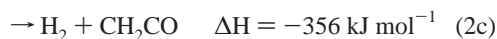
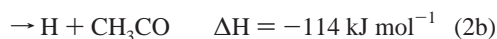


where R is a H atom or alkyl radical. When probing the HCO channel using cavity ring-down spectroscopy, they also observed that the branching ratio of channel 1a decreases rapidly with the increasing length of R. For the reactions of O(<sup>3</sup>P) with ethylene, propene, and other alkenes (including 1-C<sub>4</sub>H<sub>8</sub>, *cis*-2-C<sub>4</sub>H<sub>8</sub>, iso-C<sub>4</sub>H<sub>8</sub>, 1-C<sub>5</sub>H<sub>10</sub>, allene, 1,3-C<sub>4</sub>H<sub>6</sub>, cyclopentene, and cyclohexene), the HCO channel branching ratios were 0.71 ± 0.16, 0.05 ± 0.02, and 0, respectively.<sup>12</sup> To explain this observation, they proposed that other channels, such as the H<sub>2</sub>CO channel, tend to contribute larger fractions to the reaction as the hydrocarbon chain of the alkene molecule lengthens.

Most recently, another three studies were carried out on the reaction of the oxygen atom with the simplest alkene, C<sub>2</sub>H<sub>4</sub>. By means of IR emission spectroscopy, James et al.<sup>16</sup> observed the vibrationally excited products of HCO, H<sub>2</sub>CO, CO, and CO<sub>2</sub> from the 193 nm laser irradiation of the SO<sub>2</sub>–C<sub>2</sub>H<sub>4</sub>–Ar mixture, and they ascribed the formation of CO and CO<sub>2</sub> to the secondary reactions of O(<sup>3</sup>P) with ethylene. Their study mainly focused on the secondary reactions forming CO and CO<sub>2</sub> but did not deal with the H<sub>2</sub>CO product channel. Using the crossed molecular beam scattering technique with soft electron ionization, Casavecchia et al.<sup>17</sup> observed the exoergic channels of the O(<sup>3</sup>P) + C<sub>2</sub>H<sub>4</sub> reaction and measured the relative branching ratios to be 0.27 ± 0.06, 0.01 ± 0.005, 0.13 ± 0.03, 0.47 ± 0.09, and 0.16 ± 0.08 for the channels 2a–2e, respectively.

<sup>†</sup> Part of the "Sheng Hsien Lin Festschrift".

\* To whom correspondence should be addressed. E-mail: hongmei@iccas.ac.cn.



Interestingly, their measurement shows that a substantial amount of H<sub>2</sub>CO is formed. This is opposed to the general notion that the CH<sub>2</sub>CHO channel (2a) and the HCO channel (2d) are the only two major reaction channels of the O(<sup>3</sup>P) + C<sub>2</sub>H<sub>4</sub> reaction.<sup>18</sup> The potential energy surface of the O(<sup>3</sup>P) + C<sub>2</sub>H<sub>4</sub> reaction was theoretically investigated by Nguyen et al. using various quantum chemical methods, including G3, CBS-QB3, G2M(CC, MP2), and MRCI.<sup>19</sup> The major products (with predicted yields at *T* = 300/2000 K) were CH<sub>3</sub> + HCO (48/37%), H + CH<sub>2</sub>CHO (40/19%), and CH<sub>2</sub>(X<sup>3</sup>B<sub>1</sub>) + H<sub>2</sub>CO (5/29%). The calculation also showed that the reaction of the O(<sup>3</sup>P) with C<sub>2</sub>H<sub>4</sub> leads to the product of H<sub>2</sub>CO but the yield of the H<sub>2</sub>CO channel is relatively low at room temperature.

For larger alkenes, Oguchi et al. investigated the mechanism of reactions of O(<sup>3</sup>P) with three isomeric butenes (*trans*-2-, *iso*-, and 1-butene).<sup>20</sup> They measured the yields of the CH<sub>3</sub> and C<sub>2</sub>H<sub>5</sub> radical products using photoionization mass spectrometry. For isobutene, the fractions of CH<sub>3</sub> and C<sub>2</sub>H<sub>5</sub> channel were 0.24 ± 0.08 and 0.29 ± 0.05, respectively. The total fraction yield of the CH<sub>3</sub> and C<sub>2</sub>H<sub>5</sub> products were 0.53. For 1-butene, the total yield of the CH<sub>3</sub> and C<sub>2</sub>H<sub>5</sub> products was only 0.10. The rest of the channels accounting for a large fraction remained suspensive.

Zhao et al.<sup>21</sup> calculated the reaction pathways of the O(<sup>3</sup>P) with isobutene using the unrestricted second-order Møller–Plesset perturbation (UMP2) and complete basis set CBS-4M level of theory methods. They predicted the major product channels to be CH<sub>2</sub>C(O)CH<sub>3</sub> + CH<sub>3</sub>, *cis*-/*trans*-CH<sub>3</sub>CHCHO + CH<sub>3</sub>, (CH<sub>3</sub>)<sub>2</sub>CCO + H<sub>2</sub>, and CH<sub>3</sub>C(CH<sub>2</sub>)<sub>2</sub> + OH, among which (CH<sub>3</sub>)<sub>2</sub>CCO + H<sub>2</sub> was the energetically most favorable one. In addition, they predicted that the product channel (CH<sub>3</sub>)<sub>2</sub>C + H<sub>2</sub>CO is only of minor contribution.

To sum up, previous experimental investigations either observed directly the formation of the H<sub>2</sub>CO product<sup>16,17</sup> for the O(<sup>3</sup>P) + C<sub>2</sub>H<sub>4</sub> reaction or indicated the existence of such a channel for the reactions of O(<sup>3</sup>P) with larger alkenes.<sup>12</sup> In addition, theoretical calculations<sup>19,21</sup> predicted the H<sub>2</sub>CO channel with a minor fraction yield at room temperature. The question arises whether the H<sub>2</sub>CO product channel is common to the serial reactions of O(<sup>3</sup>P) with alkenes, and what is the mechanism underlying the formation of H<sub>2</sub>CO. In the present paper, we have investigated systematically the H<sub>2</sub>CO channel for the reactions of O(<sup>3</sup>P) with various alkenes by means of step-scan time-resolved FTIR emission spectroscopy. A general trend is observed in which the fraction yield of the H<sub>2</sub>CO product increases substantially as the reactant alkene varies from C<sub>2</sub>H<sub>4</sub>, C<sub>3</sub>H<sub>6</sub>, 1-C<sub>4</sub>H<sub>8</sub>, *iso*-C<sub>4</sub>H<sub>8</sub>, to 1-C<sub>5</sub>H<sub>10</sub>. An alternative scenario for the reaction of O(<sup>3</sup>P) with alkenes is revealed in which, as the hydrocarbon chain of the alkene molecule is lengthened, the initially formed energized intermediate ketocarbene RCH<sub>2</sub>-CHCH<sub>2</sub>O\* involves more rapid delocalization of the energy, and thus, the 3,2 H-atom shift followed by breaking of the C<sub>1</sub>-C<sub>2</sub> bond may become the dominant process which leads to the formation of the final product H<sub>2</sub>CO.

## 2. Experimental Section

The reaction products are monitored by step-scan time-resolved Fourier transform emission spectroscopy.<sup>22</sup> A step-scan FTIR spectrometer is commercially available but requires significant modification for coupling with a pulsed laser and applying it to the study of laser-initiated free-radical reactions. This newly upgraded machine comprises a Nicolet Nexus 870 step-scan FTIR spectrometer, a Lambda Physik (LPX305i) Excimer laser, and a pulse generator (Stanford Research DG535) to initiate the laser pulse and achieve synchronization of the laser with the data collection, two digitizers (internal 100 kHz 16 bit digitizer and external 100 MHz 14 bit GAGE 8012A digitizer), which offer fast time resolution and a wide dynamic range as needed, and a personal computer to control the whole experiment. The detector used in this experiment is a liquid-nitrogen-cooled InSb detector.

The reaction is initiated in a stainless steel flow reaction chamber. A pair of parallel multilayer coated mirrors (reflectivity *R* > 0.95 at 351 nm) reflect the UV laser beam multiple times to increase the photolysis zone. O(<sup>3</sup>P) atoms are produced via the laser photodissociation of NO<sub>2</sub> at 351 nm (XeF laser, Lambda Physik LPX305i, ~50 mJ cm<sup>-2</sup>). Only the ground-state O(<sup>3</sup>P) atoms are produced following the 351 nm photolysis of NO<sub>2</sub>, and there is no interference from O(<sup>1</sup>D) atoms. Typically, 250 mTorr of alkenes (≥99.5%) and 150 mTorr of NO<sub>2</sub> (≥99.9%) enter the flow chamber 1 cm above the photolysis beam via needle valves. The chamber is pumped by an 8 L s<sup>-1</sup> mechanical pump, and the stagnation pressure of the chamber is measured by a MKS capacitance monometer. The constant pressure of sample is maintained by adjusting the pumping speed and the needle valves. Transient infrared emission is collected by a pair of gold-coated White-Cell spherical mirrors and collimated by a CaF<sub>2</sub> lens to the step-scan Fourier spectrometer. The spectrometer and the collimating tube are both flushed with N<sub>2</sub> to eliminate the environmental CO<sub>2</sub> absorption. Alkenes were purchased from Aldrich and used as received.

## 3. Results and Discussion

**3.1. Identification of the Reaction Products from IR Emission Spectra.** In the first reference experiment, when pure alkenes were irradiated by a 351 nm laser, no IR emission was observed. This is expected because alkenes cannot be photolyzed by a 351 nm laser.

In the second reference experiment, when pure NO<sub>2</sub> was irradiated by a 351 nm laser, the IR emission due to the photofragment NO spanning from 1790 to 1970 cm<sup>-1</sup> was observed, as shown in Figure 1 with the three-dimensional “waterfall” view of the emission spectra at selected time delays following laser excitation of the pure NO<sub>2</sub>. Photodissociation of NO<sub>2</sub> at 351 nm produces vibrationally excited NO and the O(<sup>3</sup>P) atom



Fortunately, the NO spectral region is isolated and will not interfere with the detection of the products of O(<sup>3</sup>P) with alkenes, which usually cover the spectral region higher than 1970 cm<sup>-1</sup>.

When the flowing gaseous mixture of the O(<sup>3</sup>P) precursor, NO<sub>2</sub>, with alkenes was irradiated by a 351 nm laser, intense IR emissions were observed. As an example, Figure 2 shows the three-dimensional waterfall views of the IR emission spectra at selected time delays following laser excitation of the NO<sub>2</sub>/iso-C<sub>4</sub>H<sub>8</sub> mixture. Similarly, the time-resolved IR emission

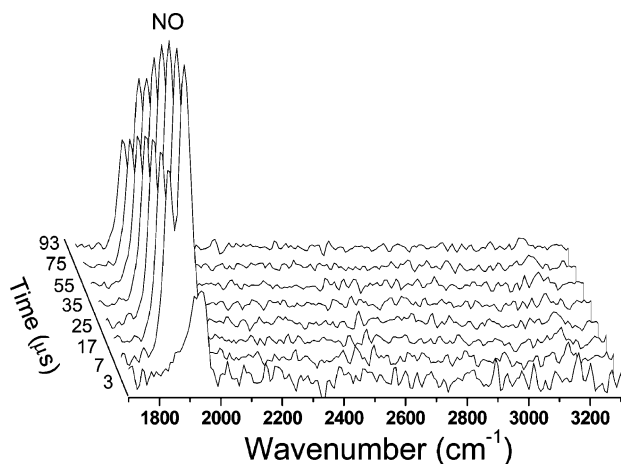


**Figure 1.** Time-resolved IR emission spectra at selected time delays of 3, 7, 17, 25, 35, 55, 75, and 93  $\mu\text{s}$  following the 351 nm photodissociation of  $\text{NO}_2$  in the 1700–3300  $\text{cm}^{-1}$  region with 16  $\text{cm}^{-1}$  resolution.

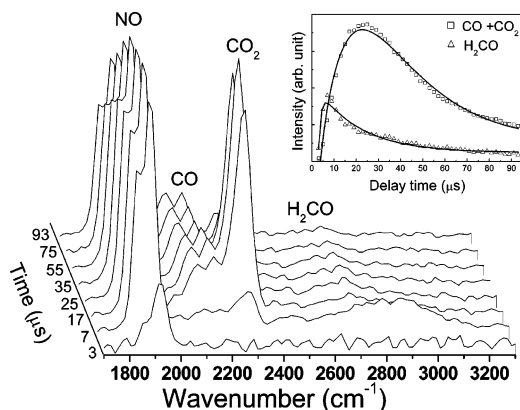


**Figure 2.** Time-resolved IR emission spectra at selected time delays of 3, 7, 17, 25, 35, 55, 75, and 93  $\mu\text{s}$  following the 351 nm irradiation of the  $\text{NO}_2$ – $\text{iso-C}_4\text{H}_8$  mixture in the 1700–3300  $\text{cm}^{-1}$  region with 32  $\text{cm}^{-1}$  resolution. The inset shows the time evolution of the peak area of the two IR emission bands of  $\text{H}_2\text{CO}$  and  $\text{CO}/\text{CO}_2$ . The triangle spots are the experimental peak area of the  $\text{H}_2\text{CO}$  emission band, and the square spots are the experimental data of the  $\text{CO}/\text{CO}_2$  emission band. The solid curves are the fitting results.

spectra were collected for the reactions of  $\text{O}(^3\text{P})$  with various alkenes including  $\text{C}_2\text{H}_4$ ,  $\text{C}_3\text{H}_6$ ,  $1\text{-C}_4\text{H}_8$ ,  $\text{iso-C}_4\text{H}_8$ ,  $1\text{-C}_5\text{H}_{10}$ , and  $1,3\text{-C}_4\text{H}_6$ . To compare explicitly the products of these reactions, the specific time slices of the IR emission spectra for various alkenes are displayed in Figure 3. The IR emissions arise from the vibrationally excited products from the reactions of  $\text{O}(^3\text{P})$  with alkenes. These reaction products can be identified from spectral assignment.

TR-FTIR emission spectra record the infrared fluorescence emitted from vibrationally excited species due to a set of vibrational transitions  $\nu \rightarrow \nu - 1$ , which consists of numerous rotational transitions. Therefore, the IR emission band is generally much broader than normal static IR absorption spectra, and the peak center exhibits a somewhat red shift relative to the fundamental frequency position ( $1 \rightarrow 0$ ). Collected with a spectral resolution of 16  $\text{cm}^{-1}$ , only the contour due to the numerous overlapping rovibrational transitions can be obtained. The rotational structure cannot be resolved.

Judging from its spectral position, the emission band spanning from 2050 to 2380  $\text{cm}^{-1}$  is attributed to the overlapping CO emission (fundamental band at 2143  $\text{cm}^{-1}$ ) and  $\text{CO}_2$  emission (fundamental band at 2349  $\text{cm}^{-1}$ ). As will be discussed, CO and  $\text{CO}_2$  are formed mainly from the secondary reactions of

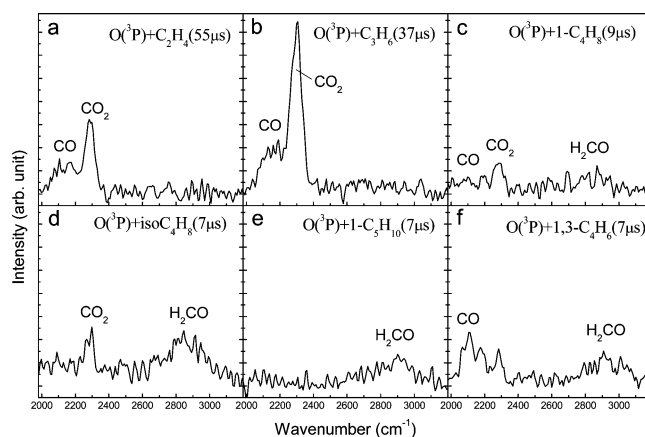


**Figure 3.** IR emission spectra for the reactions of  $\text{O}(^3\text{P})$  with six different alkenes at typical reaction times: (a)  $\text{C}_2\text{H}_4$ , (b)  $\text{C}_3\text{H}_6$ , (c)  $1\text{-C}_4\text{H}_8$ , (d)  $\text{iso-C}_4\text{H}_8$ , (e)  $1\text{-C}_5\text{H}_{10}$ , and (f)  $1,3\text{-C}_4\text{H}_6$ . Figure 3a and b shows the spectra at the reaction time when the  $\text{CO}/\text{CO}_2$  bands reach their maximum intensity. Figure 3c–f shows the spectra at the reaction time when the  $\text{H}_2\text{CO}$  band reaches its maximum intensity.

$\text{O}(^3\text{P}) + \text{alkenes}$ . Another broad emission band from 2600 to 3100  $\text{cm}^{-1}$  is assigned to both vibrationally excited  $\text{H}_2\text{CO}$   $\Delta\nu_5 = -1$  (b-type  $\text{CH}_2$  asymmetric stretch mode: 2843  $\text{cm}^{-1}$ )<sup>23</sup> and  $\Delta\nu_1 = -1$  (a-type  $\text{CH}_2$  symmetric stretch mode: 2783  $\text{cm}^{-1}$ )<sup>23</sup> bands. Although falling into the same spectral region, this band is not likely arising from other possible products such as  $\text{CH}_3$  (a'-type  $\text{CH}$  stretch mode: 3004  $\text{cm}^{-1}$ )<sup>23</sup> or  $\text{C}_2\text{H}_5$  (a'-type  $\text{CH}$  stretch mode: 2854  $\text{cm}^{-1}$ ; a'-type  $\text{CH}_2$  symmetric stretch mode: 3037  $\text{cm}^{-1}$ ; a'-type  $\text{CH}_3$  symmetric stretch mode: 2875  $\text{cm}^{-1}$ )<sup>23</sup>. It is known that the dominant reaction channels of  $\text{O}(^3\text{P}) + \text{C}_2\text{H}_4$  and  $\text{O}(^3\text{P}) + \text{C}_3\text{H}_6$  are to form  $\text{CH}_3$  and  $\text{C}_2\text{H}_5$ .<sup>12,18</sup> However, as shown in Figure 3a and b, no emission signals can be observed in the spectral region (2600–3100  $\text{cm}^{-1}$ ) where  $\text{CH}_3$  or  $\text{C}_2\text{H}_5$  should be present. On the other hand, it has been observed that the fraction yield of the  $\text{CH}_3$  and  $\text{C}_2\text{H}_5$  channel decreases with the increasing size of the alkene molecule.<sup>12</sup> Therefore, if no  $\text{CH}_3$  or  $\text{C}_2\text{H}_5$  is observed for the  $\text{O}(^3\text{P}) + \text{C}_2\text{H}_4$  and  $\text{O}(^3\text{P}) + \text{C}_3\text{H}_6$  reactions in the IR emission spectra, there are no chances for observing the  $\text{CH}_3$  or  $\text{C}_2\text{H}_5$  emission for the reaction of  $\text{O}(^3\text{P})$  with larger alkenes. The emission bands from 2600 to 3100  $\text{cm}^{-1}$  observed in Figure 3c–e are arising from other reaction products, most likely,  $\text{H}_2\text{CO}$ . James et al. also observed and assigned this emission band to the  $\nu_1$  and  $\nu_5$  vibrationally excited  $\text{H}_2\text{CO}$  when studying the reaction of  $\text{O}(^3\text{P})$  with  $\text{C}_2\text{H}_4$ .<sup>16</sup> The reason why no IR emissions from the  $\text{CH}_3$  or  $\text{C}_2\text{H}_5$  were observed should be due to their small Einstein A coefficient [ $\text{CH}_3$  (7.5  $\text{s}^{-1}$ )<sup>24</sup> or their low vibrational excitation. In contrast, the Einstein A coefficient of  $\text{H}_2\text{CO}$  is large (73.2  $\text{s}^{-1}$  for  $\nu_1$  and 88.6  $\text{s}^{-1}$  for  $\nu_5$ ).<sup>25</sup> IR emission spectroscopy is thus a sensitive probe for  $\text{H}_2\text{CO}$  but not for  $\text{CH}_3$  and  $\text{C}_2\text{H}_5$ .

**3.2. Identification of  $\text{H}_2\text{CO}$  as the Primary Product and  $\text{CO}/\text{CO}_2$  as the Secondary Products of the  $\text{O}(^3\text{P}) + \text{Alkene}$  Reactions.** The inset in Figure 2 plots the IR emission intensity of the peak area as a function of the reaction time. The rise reflects the product formation, and the decay is due to vibrational relaxation and removal from the observation zone. The diffusion effect causing the removal from the observation zone can be neglected on the time scale of hundreds of microseconds.<sup>26</sup> Therefore, the rise and fall of the IR emission temporal curves are fitted with a sum of two exponentials  $y_0 + C(\exp(-k_1t) - \exp(-k_2t))$ , providing information on the kinetics of the product formation and vibrational relaxation. The typical fitting results are shown in the inset of Figure 2. Satisfactory fitting results are obtained although the model is greatly simplified without

considering complications such as product molecules populated at ground vibrational level ( $\nu = 0$ ) not being detected by IR emission spectroscopy.<sup>27</sup>

It is estimated that only a small amount (approximately 5%) of NO<sub>2</sub> molecules are dissociated upon 351 nm laser irradiation at a power of 50 mJ cm<sup>-2</sup>, leading to [O(<sup>3</sup>P)]  $\approx 2 \times 10^{14}$  molecules/cm<sup>3</sup>. The concentration range of [iso-C<sub>4</sub>H<sub>8</sub>] =  $3 \times 10^{15}$ – $1 \times 10^{16}$  molecules/cm<sup>3</sup> is sufficiently in excess to ensure pseudo-first-order conditions. The rate of the rise of product formation from the reaction of O(<sup>3</sup>P) with iso-C<sub>4</sub>H<sub>8</sub> is therefore given by  $k' = k[\text{iso-C}_4\text{H}_8]$ . The biexponential fitting yields a formation rate constant of  $8.5 \times 10^{-12}$  cm<sup>3</sup> molecule<sup>-1</sup> s<sup>-1</sup> for H<sub>2</sub>CO and  $3.4 \times 10^{-12}$  cm<sup>3</sup> molecule<sup>-1</sup> s<sup>-1</sup> for CO/CO<sub>2</sub>. The formation rate constant of H<sub>2</sub>CO agrees well with the reported overall rate constant of  $1.8 \times 10^{-11}$  cm<sup>3</sup> molecule<sup>-1</sup> s<sup>-1</sup> for the reaction of O(<sup>3</sup>P) with iso-C<sub>4</sub>H<sub>8</sub>.<sup>28</sup> Consequently, H<sub>2</sub>CO can be concluded to be the primary reaction product from the O(<sup>3</sup>P) + iso-C<sub>4</sub>H<sub>8</sub> reaction. In contrast, the formation of CO/CO<sub>2</sub> lags behind that of H<sub>2</sub>CO, corresponding to a rate constant of  $3.4 \times 10^{-12}$  cm<sup>3</sup> molecule<sup>-1</sup> s<sup>-1</sup>, which is much smaller than the overall reaction rate constant of O(<sup>3</sup>P) with iso-C<sub>4</sub>H<sub>8</sub>. This indicates that CO and CO<sub>2</sub> are most likely produced from secondary reactions of O(<sup>3</sup>P) + alkenes, that is, the consecutive reaction of the primary products causing the formation delay of CO/CO<sub>2</sub>. Previous investigations also show that a negligible amount of CO is produced directly from the reactions of O(<sup>3</sup>P) + alkenes.<sup>11,17,20</sup> Similar kinetics analysis is applied to the other O(<sup>3</sup>P) + alkene reactions, and it all shows that H<sub>2</sub>CO is the primary product and CO/CO<sub>2</sub> are secondary products.

**3.3. Possible Secondary Reactions.** Although it is a versatile and powerful means of observing the IR-active products in a reaction mixture, the IR emission detection has the disadvantage of low sensitivity relative to other detection methods. Thus, the species' partial pressures are necessarily relatively high to ensure adequate signal-to-noise ratios for detection purposes. Under these conditions, secondary chemistry usually plays a role in the production of IR-active species.

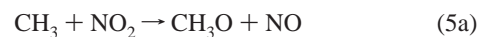
The primary reactions of O(<sup>3</sup>P) + alkenes lead to some radical products, including CH<sub>3</sub>, C<sub>2</sub>H<sub>5</sub>, CH<sub>2</sub>CHO, HCO, and H atoms. Due to the low concentration of these radicals, secondary radical–radical reactions are negligible, while secondary reactions of the abundant alkene or NO<sub>2</sub> molecules with these primary radicals such as CH<sub>3</sub> + NO<sub>2</sub>, CH<sub>2</sub>CHO + NO<sub>2</sub>, HCO + alkenes, and HCO + NO<sub>2</sub> are likely to contribute to the formation of the observed IR-active products and have to be considered.

The first IR-active product H<sub>2</sub>CO has been identified to be generated from the primary reactions of O(<sup>3</sup>P) + alkenes by kinetics analysis. Still, the following possible secondary reactions are considered and eliminated as a source for generating H<sub>2</sub>CO. The reaction of HCO + alkenes can be ruled out due to its extremely small reactivity ( $k$  on the order of  $10^{-17}$  cm<sup>3</sup> molecule<sup>-1</sup> s<sup>-1</sup><sup>29</sup>). The CH<sub>2</sub>CHO + NO<sub>2</sub> reaction does not produce H<sub>2</sub>CO but proceeds through other pathways, as suggested by Barnhard et al.'s study<sup>30</sup>



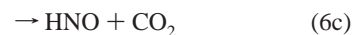
The CH<sub>3</sub> + NO<sub>2</sub> reaction only produces a negligible amount of H<sub>2</sub>CO. Yamada,<sup>31</sup> Wollenhaupt,<sup>32</sup> and Biggs<sup>33</sup> have identified the reaction channels 5a, 5b, and 5c, but none of these studies have observed the product H<sub>2</sub>CO from the reaction of CH<sub>3</sub> + NO<sub>2</sub>. The theoretical calculation by Biggs<sup>33</sup> predicted that the

H<sub>2</sub>CO channel yielded from CH<sub>3</sub> + NO<sub>2</sub> is a factor of 50 smaller than the major CH<sub>3</sub>O channel (5a)



For the other observed IR-active products CO and CO<sub>2</sub>, the kinetics analysis already shows that they are due to the secondary reactions of O(<sup>3</sup>P) + alkenes. After analyzing the expected products of possible secondary reactions, it is found that the reaction of HCO + NO<sub>2</sub> is the most probable secondary reaction for generating the products of CO and CO<sub>2</sub>.

HCO radicals are known to react with NO<sub>2</sub> rapidly with a rate constant of  $2.7$ – $5.7 \times 10^{-11}$  cm<sup>3</sup> molecule<sup>-1</sup> s<sup>-1</sup>.<sup>34</sup> Recently, Meyer et al.<sup>35</sup> experimentally studied the products of the reaction of HCO with NO<sub>2</sub>, suggesting seven reaction channels



Due to the dissociation of HCO<sub>2</sub> to form H and CO<sub>2</sub> with only a low activation barrier, the reaction channel 6e is, in effect, indistinguishable from 6d. The branching ratios yielding CO and CO<sub>2</sub> were found to be  $(k_{6a} + k_{6b})/k_6 = (0.66 \pm 0.10)$  and  $(k_{6c} + k_{6d} + k_{6e})/k_6 = (0.34 \pm 0.10)$ , respectively. Rim et al. also measured the branching ratios forming CO + NO + OH and H + NO + CO<sub>2</sub> to be  $63 \pm 5$  and  $37 \pm 5\%$ , respectively.<sup>34</sup> Guo et al.<sup>36</sup> determined the yield fractions of CO<sub>2</sub> to be  $52 \pm 10\%$  and estimated that of CO to be  $48 \pm 10\%$  from the HCO + NO<sub>2</sub> reaction. All of these studies have identified that the reaction of HCO + NO<sub>2</sub> produces dominantly CO and CO<sub>2</sub>. Since HCO is also a major primary product from O(<sup>3</sup>P) + alkenes reactions, the secondary reaction of HCO + NO<sub>2</sub> is the most probable source for generating CO and CO<sub>2</sub> observed in the IR emission spectra.

Although we are targeting our study to the reaction of O(<sup>3</sup>P) + alkenes in this work, the secondary reactions cannot be avoided because of the presence of the reactive primary radical products, that is, HCO in this case, to react with NO<sub>2</sub>, forming observable products of CO and CO<sub>2</sub>. On the other hand, the products CO and CO<sub>2</sub> are presumably mainly correlated with the primary HCO channel from the O(<sup>3</sup>P) + alkene reactions. We can therefore elucidate the relative yield of the HCO channel by measuring the yield of CO and CO<sub>2</sub>.

**3.4. The Relative Yield of the H<sub>2</sub>CO Channel to the HCO Channel.** In the O(<sup>3</sup>P) + alkenes reactions, as the hydrocarbon chain lengthens from C<sub>2</sub>H<sub>4</sub>, C<sub>3</sub>H<sub>6</sub>, 1-C<sub>4</sub>H<sub>8</sub>, iso-C<sub>4</sub>H<sub>8</sub>, to 1-C<sub>5</sub>H<sub>10</sub>, one obvious trend can be observed from Figure 3 in which the fraction yield of the H<sub>2</sub>CO channel relative to the HCO channel (reflected by the CO/CO<sub>2</sub> emission intensity in the spectra)



**TABLE 2: Possible Underlying Factors Leading to the Preference of the Hydrogen Atom Migration Process Involved in the Reactions of O(<sup>3</sup>P) with Alkenes**

alkene	exothermicity <sup>a</sup>	R group causing steric hindrance for the 1,2 H-atom shift <sup>b</sup>	C <sub>3</sub> -H bond energy of the alkene <sup>c,37</sup>
CH <sub>2</sub> =CH <sub>2</sub>	-19.8	H	
CH <sub>3</sub> -CH=CH <sub>2</sub>	-325.4	CH <sub>3</sub>	369
CH <sub>3</sub> CH <sub>2</sub> -CH=CH <sub>2</sub>	-337.9	CH <sub>3</sub> CH <sub>2</sub>	350.6
(CH <sub>3</sub> ) <sub>2</sub> -C=CH <sub>2</sub>	-320.9	(CH <sub>3</sub> ) <sub>2</sub>	362.8
CH <sub>3</sub> (CH <sub>2</sub> ) <sub>2</sub> -CH=CH <sub>2</sub>	-336.6	CH <sub>3</sub> CH <sub>2</sub> CH <sub>2</sub>	345.2

<sup>a</sup> Exothermicity (in kJ mol<sup>-1</sup>) of the H<sub>2</sub>CO channel of the O + alkene reaction; the enthalpies of formation originated from ref 38. <sup>b</sup> Steric hindrance effect caused by the group attached to the C2 atom of the hot diradical, RCHCH<sub>2</sub>O. <sup>c</sup> C<sub>3</sub>-H bond energy of the alkene, in kJ mol<sup>-1</sup>.

for the 1,2 H-atom shift is expected to increase with the increasing size of the R group. As a result, the 1,2 H-atom shift process which leads to the HCO channel becomes less and less important for longer-chain alkenes. Alternatively, the 3,2 H-atom shift process takes over, and the H<sub>2</sub>CO channel plays a more significant role. In fact, the observed trend of the increasing yield of H<sub>2</sub>CO with longer-chain alkenes agrees quite well with the variation of the steric hindrance.

The allylic C<sub>3</sub>-H bond energy decreases when the alkene goes from C<sub>3</sub>H<sub>6</sub> and 1-C<sub>4</sub>H<sub>8</sub> to 1-C<sub>5</sub>H<sub>10</sub>, as shown in Table 2. Since the 3,2 H-atom shift process somehow involves the cleavage of the C<sub>3</sub>-H bond first, it is expected that the weaker the C<sub>3</sub>-H bond is, the more easily the 3,2 H-atom shift occurs and, thus, the more product of H<sub>2</sub>CO yielded. Thus, the H<sub>2</sub>CO yield is increased from C<sub>3</sub>H<sub>6</sub> and 1-C<sub>4</sub>H<sub>8</sub> to 1-C<sub>5</sub>H<sub>10</sub>. On the other hand, the allylic C<sub>3</sub>-H bond energy is not the only factor causing the variation of the H<sub>2</sub>CO yield with alkenes. For instance, the C<sub>3</sub>-H bond energy of iso-C<sub>4</sub>H<sub>8</sub> is between those of C<sub>3</sub>H<sub>6</sub> and 1-C<sub>4</sub>H<sub>8</sub>, but its H<sub>2</sub>CO yield exceeds any of them. This indicates that the factor of steric hindrance plays a more significant role. For the iso-C<sub>4</sub>H<sub>8</sub> reaction compared to those of C<sub>3</sub>H<sub>6</sub> and 1-C<sub>4</sub>H<sub>8</sub>, the (CH<sub>3</sub>)<sub>2</sub> group presumably generates much larger steric hindrance for the competing 1,2 H-atom shift channel and thus leads to the increasing yield of the H<sub>2</sub>CO channel.

In summary, an overall scenario can be revealed for the formation of the H<sub>2</sub>CO products. There exists a H<sub>2</sub>CO channel for the O(<sup>3</sup>P) + alkene reactions, and the fraction yield of this channel increases as the hydrocarbon chain of the alkene lengthens (from C<sub>2</sub>H<sub>4</sub>, C<sub>3</sub>H<sub>6</sub>, 1-C<sub>4</sub>H<sub>8</sub>, iso-C<sub>4</sub>H<sub>8</sub>, to 1-C<sub>5</sub>H<sub>10</sub>). This channel might occur via a 3,2 H-atom shift in the energized adduct



followed by breaking of the C<sub>1</sub>-C<sub>2</sub> bond. Opposed to the normally proposed 1,2 H-atom shift



followed by the formation of the radical HCO channel, the 3,2 H-atom shift mechanism shows obvious preference as the chain of the alkene lengthens. The reaction exothermicity, structural steric hindrance, and allylic C<sub>3</sub>-H bond energy are possible factors causing the bias of the 3,2 H-atom shift over the 1,2 H-atom shift involved in the O(<sup>3</sup>P) + alkene reactions.

The mechanism we proposed here for the formation of H<sub>2</sub>CO via a 3,2 H-atom shift is more straightforward and can explain well the experimentally observed trend of the H<sub>2</sub>CO

yield varying with alkenes. It is therefore desirable to perform some ab initio calculations to explore the feasibility of this mechanism. Also, interesting questions would emerge such as on which surface would the H<sub>2</sub>CO channel occur, the triplet or singlet, and whether the 3,2 H-atom shift process would need to surmount a high-energy barrier on the triplet surface, but the barrier is significantly lowered on the singlet surface just like the already-known behavior of the 1,2 H-shift process. We hope this experimental paper can arouse further related computational studies.

**Acknowledgment.** This work is financially supported by the National Natural Science Foundation of China (Grant No. 20473100 and No. 20673126), the National Basic Research Program of China, and the Chinese Academy of Sciences.

## References and Notes

- Glassman, I. *Combustion*, 2nd ed.; Academic Press: FL, 1987.
- Gardiner, W. C., Jr. *Combustion Chemistry*; Springer-Verlag: New York, 1984.
- Nguyen, T. L.; Peeters, J.; Vereecken, L. *J. Phys. Chem. A* **2006**, *110*, 12166.
- Cvetanovic, R. J. *J. Chem. Phys.* **1955**, *23*, 1375.
- Cvetanovic, R. J. *Can. J. Chem.* **1955**, *33*, 1684.
- Cvetanovic, R. J. *J. Chem. Phys.* **1956**, *25*, 376.
- Cvetanovic, R. J. *J. Chem. Phys.* **1959**, *30*, 19.
- Cvetanovic, R. J. *J. Chem. Phys.* **1960**, *33*, 1063.
- Cvetanovic, R. J. *J. Phys. Chem.* **1970**, *74*, 2730.
- Cvetanovic, R. J. *Adv. Photochem.* **1963**, *1*, 115.
- Quandt, R.; Min, Z.; Wang, X.; Bersohn, R. *J. Phys. Chem. A* **1998**, *102*, 60.
- Min, Z.; Wong, T. H.; Quandt, R.; Bersohn, R. *J. Phys. Chem. A* **1999**, *103*, 10451, and references therein.
- Min, Z.; Wong, T. H.; Su, H.; Bersohn, R. *J. Phys. Chem. A* **2000**, *104*, 9941.
- Su, H.; Bersohn, R. *J. Chem. Phys.* **2001**, *115*, 217.
- Su, H.; Bersohn, R. *J. Phys. Chem. A* **2001**, *105*, 9178.
- James, A. D.; Eunsook, S. H.; Karen, J. C.; Gary, D. D. *J. Phys. Chem. A* **2004**, *108*, 10965.
- Casavecchia, P.; Capozza, G.; Segoloni, E.; Leonori, F.; Balucani, N.; Gualberto, G. *J. Phys. Chem. A* **2005**, *109*, 3527.
- Schmoltner, A. M.; Chu, P. M.; Brudzynski, R. J.; Lee, Y. T. *J. Chem. Phys.* **1989**, *91*, 6926.
- Nguyen, T. L.; Vereecken, L.; Hou, X. J.; Nguyen, M. T.; Peeters, J. *J. Phys. Chem. A* **2005**, *109*, 7489, and reference therein.
- Oguchi, T.; Ishizaki, A.; Kakuta, Y.; Matsui, H. *J. Phys. Chem. A* **2004**, *108*, 1409.
- Zhao, H. M.; Bian, W. S.; Liu, K. *J. Phys. Chem. A* **2006**, *110*, 7858.
- Zhu, Q.; Huang, S.; Wang, X. *Chin. J. Chem. Phys.* **1993**, *6*, 87.
- NIST Standard Reference Database 69, NIST Chemistry WebBook. <http://webbook.nist.gov/chemistry/> (June 2005 release).
- Donaldson, D. J.; Stephen, R. L. *J. Chem. Phys.* **1986**, *85*, 817.
- Zou, P.; Klippenstein, S. J.; Osborn, D. L. *J. Phys. Chem. A* **2005**, *109*, 4921.
- Xiang, T.; Liu, K.; Shi, C.; Su, H.; Kong, F. *Chem. Phys. Lett.* **2007**, *437*, 8.
- Osborn, D. L. *J. Phys. Chem. A* **2003**, *107*, 3728.
- Adusei, G. Y.; Fontijn, A. *J. Phys. Chem.* **1994**, *98*, 3732.
- Lesclaux, R.; Roussel, P.; Veyret, B.; Pouchan, C. *J. Am. Chem. Soc.* **1986**, *108*, 3872.
- Barnhard, K. I.; Santiago, A.; He, M.; Asmar, F.; Weiner, B. R. *Chem. Phys. Lett.* **1991**, *178*, 150.
- Yamada, F.; Slage, I. R.; Gutman, D. *Chem. Phys. Lett.* **1981**, *83*, 409.
- Wollenhaupt, M.; Crowley, J. N. *J. Phys. Chem. A* **2000**, *104*, 6429.
- Biggs, P.; Canosa-Mas, C. E.; Fracheboud, J.-M.; Parr, A. D.; Shallcross, D. E.; Wayne, R. P. *J. Chem. Soc., Faraday Trans.* **1993**, *89*, 4163.
- Rim, K. T.; Hershberger, J. F. *J. Phys. Chem. A* **1998**, *102*, 5898, and references therein.
- Meyer, St.; Temps, F. *Int. J. Chem. Kinet.* **2000**, *32*, 136.
- Guo, Y.; Smith, S. C.; Moore, C. B. *J. Phys. Chem.* **1995**, *99*, 7473.
- Lide, D. R. *CRC Handbook of Chemistry and Physics*, 85th ed.; CRC Press: Boca Raton, FL, 2004.
- Luo, Y. R. *Handbook of Bond Energies* (in Chinese); Science Press: Beijing, China, 2005.